Cationic Residues 53 and 56 Control the Anion-Induced Interfacial k^*_{cat} Activation of Pancreatic Phospholipase A_2†

Joseph Rogers,‡ Bao-Zhu Yu,‡ Ming-Daw Tsai,§ Otto G. Berg,*,|| and Mahendra Kumar Jain*,‡

Department of Chemistry and Biochemistry, University of Delaware, Newark, Delaware 19716, Departments of Chemistry and Biochemistry and Ohio State Biochemistry Program, The Ohio State University, Columbus, Ohio 43201, and Department of Molecular Biology, Uppsala University Biomedical Center, Uppsala, Sweden

Received November 26, 1997; Revised Manuscript Received March 16, 1998

ABSTRACT: Added NaCl or anionic amphiphiles increase the rate of hydrolysis of dispersions of zwitterionic phospholipid by pancreatic phospholipase A_2 (PLA2). Two effects of the negative charge at the interface have been dissected: enhanced binding of the enzyme to the interface, and k^*_{cat} activation of the enzyme at the interface [Berg et al. (1997) *Biochemistry 36*, 14512−14530]. Results reported here show that the structural basis for the k^*_{cat} activation is predominantly through cationic K53 and K56 in bovine pancreatic PLA2 with the anionic interface. The maximum rate at saturating diheptanoylphosphatidylcholine micelles, V_M^{app}, for WT, K56M, and K53M in 4 M NaCl is in the 800−1300 s^{-1} range. In contrast, V_M^{app} at 0.1 M NaCl is considerably higher for K56M (400 s^{-1}) and K53M (230 s^{-1}) compared to the rate with WT (30 s^{-1}) or K56E (45 s^{-1}). The rate of hydrolysis of anionic dimyristoylphosphatidylmethanol vesicles is virtually the same with all these mutants (200−300 s^{-1}) and it is not affected by added NaCl. The chemical step for the hydrolysis of anionic and zwitterionic substrates remains rate-limiting in the presence or absence of added NaCl. A modest (≃10-fold) effect of K56M substitution or of added NaCl is seen on the binding of the enzyme to the interface; however, the binding of the substrate or a substrate mimic to the active site of the enzyme at the interface is not affected by more than a factor of 2. Magnitudes of the primary rate and equilibrium parameters at the zwitterionic and anionic interfaces show that the effect of mutation or of added NaCl is primarily on k^*_{cat} at the zwitterionic interface. These results are interpreted in terms of a two-state model for the interfacial allosteric activation, where the enzyme−substrate complex at the zwitterionic interface becomes catalytically active only after the positive charge on cationic K56 and K53 has been removed by mutation or neutralized by anionic charges in the interface.

Regulation of the catalytic behavior of an enzyme by an interface is a problem of general interest in membrane biochemistry, and it assumes particular relevance for the lipolytic enzymes (*1*). Toward this goal, we have formulated the consequences of interfacial catalysis and activation (*2*) by secreted phospholipase A_2 (PLA2)[1] and analyzed the kinetics in terms of the primary rate and equilibrium parameters (Scheme 1) with well-established enzymological significance (*3*, *4*). Three intrinsic factors with kinetic consequences (Scheme 1) are clearly resolved (*4*−*6*):

Scheme 1[a]

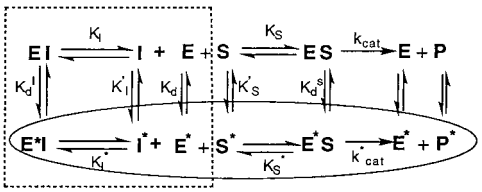

[a] Rate and equilibrium parameters at the interface (marked with an asterisk) and the aqueous phase (without an asterisk) are defined according to standard nomenclature and Michelis−Menten convention. Enzyme-mediated catalytic turnover occurs at the interface (through E* and E*S) and through the decomposition of solitary ES complex. Steps shown in the oval describe catalytic turnover in the scooting mode (*3*). Rate-limiting steps, k_{cat} and k^*_{cat}, are the rate constants for decomposition of ES and E*S, respectively. For details see ref *6*.

(a) Anionic charge at the interface promotes the binding of PLA2 to the interface (*2*, *3*, *7*). Interfacial anionic charge can be induced by anionic substrates or with anionic amphiphiles (e.g., bile salts) codispersed with zwitterionic substrate. Also, enhanced binding seen in the presence of high [NaCl] is largely due to hydrophobic effect (salting out), with an electrostatic contribution due to preferential partitioning of chloride over sodium (*8*).

† This work was supported by the U.S. Public Health Service (Grants GM29703 to M.K.J. and GM41788 to M.-D.T.) and Swedish Natural Science Research Council (to O.G.B.).

‡ University of Delaware.

§ The Ohio State University.

|| Uppsala University Biomedical Center.

[1] Abbreviations: cmc, critical micelle concentration; DC_nPC, 1,2-diacyl-*sn*-3-glycerophosphocholine with *n* carbons in each chain; DC_n-PC-ether, 1,2-dialkyl-*sn*-3-glycerophosphocholine with n carbons in each chain; DC_8PM, 1,2-dioctanoylglycero-*sn*-3-phosphomethanol; deoxy-LPC, 1-hexadecylpropanediol-3-phosphocholine; dithio-DC_7PC, 1,2-dihepatanoyl-1,2-propanedithiol-3-phosphocholine; DTNB, 5,5′-dithiobis-(2-nitrobenzoic acid); DTPC, 1,2-ditetradecylphosphatidylcholine; L, is defined as an active-site-directed substrate mimic such as substrate, product, or a competitive inhibitor; LPC_n, 1-acyl-2-lysophosphatidylcholine of indicated chain length; MJ33, 1-hexadecyl-3-(trifluoroethyl)-*rac*-glycero-2-phosphomethanol; PLA2, phospholipase A_2 from bovine pancreas unless noted otherwise; PNBr, *p*-nitrophenacyl bromide (2-bromo-4′-nitroacetophenone); POPC, 1-palmitoyl-2-oleoyl-*sn*-3-glycerophosphocholine; ppPLA2, phospholipase A_2 from pig pancreas.

S0006-2960(97)02896-1 CCC: $15.00
Published on Web 06/11/1998

Scheme 2: Two-Step Sequence for k^*_{cat} Activation by the Interfacial Anionic Charge (A*) through a Shift in the Equilibrium toward the Active Michaelis Complex, $(E^*S)_a$[a]

$$E^* + S \overset{K_1}{\rightleftharpoons} (E^*S)_i \,(+ A^*) \overset{K_2}{\rightleftharpoons} (E^*S)_a \xrightarrow{k^{**}} E^* + P$$

[a] In this model the observed rate $v = X_S k^*_{cat}/(X_S + K_M^*)$, where $k^*_{cat} = K^{**}/(1 + K_2)$ and $K^*_M = K_S = K_1K_2/(1 + K_2)$. These relations hold under the assumption that k^{**} is less than the rates involved in K_1 and K_2, i.e., k^{**} is rate-limiting. The salt effect, or the effect of the interfacial anion A*, is assumed to reside in K_2. For the anion-dependent k^*_{cat} and anion-independent K_M^*, $K_2 \gg 1$. Thus the activated state is always very rare, even at high salt. This model requires that some rate-limiting reaction intermediate, possibly the transition state (TS), is stabilized by the anion.

(b) Enhanced rate of hydrolysis of zwitterionic substrates by bound ppPLA2 at high [NaCl] (*9*) is attributed to k^*_{cat} activation by the interfacial anionic charge.

(c) The intrinsic affinity of E* for a substrate or mimic in the interface is higher than that for the enzyme in the aqueous phase.

In addition, apparent rate enhancement, by increased rate of substrate replenishment under a variety of conditions (*10*−*14*), is seen if the rate is limited by the local substrate depletion. The initial mole fraction of the substrate, X_S, that the bound enzyme "sees" is the same as the average mole fraction. However, in the absence of rapid substrate replenishment on the time scale of the intrinsic turnover, local X_S decreases rapidly, even though bulk of the substrate is not hydrolyzed. Such a departure from the local steady state follows from the fact that PLA2 with an intrinsic rate of >100 s^{-1} can hydrolyze all the substrate molecules in a micelle (typically <100) in less than a second.

In this paper we show that the structural basis for the anion-induced k^*_{cat} activation lies predominantly in residues K53 and K56 of PLA2. Although 22% of the residues are different in bovine and pig PLA2 (*15*), their structures are virtually identical to the crystal structure of K56M (*16*). Preliminary kinetic characterization suggested a noticeable effect of K56 and K53 substitutions (*16*−*18*); however, a basis for such effects could not be established. In this paper we analyze the role of K53 and K56 substitutions on the primary interfacial kinetic processes. The WT and mutants at the zwitterionic and anionic interface bind substrate mimics with comparable affinities. Surprisingly, the interfacial catalytic turnover by K53M and K56M at the zwitterionic interface is significantly higher than WT in the absence of the salt but not at high [NaCl]. These and other results suggest that K53 and K56 must play a critical role in k^*_{cat} activation of WT by the anionic charge at the interface, without a significant effect on the other parameters. Results are interpreted by a two-state model (Scheme 2) where the catalytically inert interfacial Michaelis complex, $[E^*S]_i$, at the zwitterionic interface is converted to the active $[E^*S]_a$ form by the interfacial anionic charge (A*).

EXPERIMENTAL PROCEDURES

Sources of reagents and most analytical and experimental protocols have been described before (*3*−*7*), and only salient details are given below. Construction, X-ray structure, and preliminary kinetic results with K53 and K56 substitution mutants of PLA2 has been described (*16*). DC_nPCs and the corresponding ethers (custom synthesis) were from Avanti Polar Lipids. MJ33 (*17*), dithio-DC_7PC (*14*), and DC_nPM and DC_{14}PC-ether (*19*) were synthesized as before. RM3 was kindly provided by Dr. Ronald Magolda (DuPont, Wilmington, DE). All other reagents were analytical grade. Uncertainty in measured values is 10%, and that in the derived parameters is 30%.

Kinetic Protocols. Kinetic measurements were carried out in 1 mM $CaCl_2$ and 1 mM NaCl at 25 °C and pH 8.0 under a stream of nitrogen by the pH-stat method using a Brinkman (Metrohm) or a Radiometer titrator with 3 mM NaOH titrant (*3*, *6*). Reaction progress was recorded on a strip chart recorder. Stock dispersions of DC_nPC or other lipids in water were added to the reaction mixture and equilibrated. Necessary corrections were made for the background pH drift in the absence of the enzyme. The reaction was initiated by the addition of PLA2 (0.1−30 pmol); the amount used varied depending on the observed rate. Hydrolysis commenced in less than 3 s after the addition of enzyme. The observed rate varied linearly with the amount of enzyme. Inhibitor and other components, if present in the reaction mixture, were added before or after initiating the reaction. Results in the presence of 4 M NaCl have been corrected for a small change in the titration efficiency determined by adding a known amount of myristic acid or octanoic acid to the reaction mixture in the absence of PLA2. Controls showed that the sequence of addition of substrate or PLA2 does not noticeably affect the apparent parameters, K_M^{app} and V_M^{app}. Initial rates and all the rate parameters are expressed as turnover number per second. Rates of hydrolysis of dithio-DC_7PC for the inhibition studies (e.g., Figure 8) were also monitored by coupled reaction of the thio-lysoPC with DTNB. Although rates were comparable to those obtained by the pH-stat method, the background turbidity changes suggested anomalous phase behavior.

Binding of Active-Site-Directed Mimics to PLA2. The time course of inactivation of PLA2 by PNBr, which covalently modifies the catalytic residue, His-48, provides a quantitative measure of the occupancy of the active site (*7*, *19*−*21*). The inactivation half-times obtained under appropriate conditions permit determination of the equilibrium dissociation constants for the mimic bound to the active site of E or E* form of PLA2, defined as K_L or K_L^*, respectively. The 0.03 mL alkylation reaction mixture in a 6 × 50 mm borosilicate glass tube consisted of 0.1−1 μM PLA2 in 50 mM cacodylate buffer at pH 7.3, 0.1 M NaCl, 0.5 mM $CaCl_2$, 0.03 mg of γ-globulin, and 2 mM PNBr at 23 °C. For K_L^* determinations, the incubation mixture also contained the mimic and 1.65 mM deoxy-LPC as the neutral diluent. Recall that a neutral diluent provides a micellar interface for the binding of PLA2, but individual deoxy-LPC molecules do not bind to the active site of the bound enzyme. At various time intervals, an aliquot of the incubation mixture containing 0.01−10 pmol of enzyme was added to 1.5 mL of fluorescent lipid assay solution containing 1 μg of 1-palmitoyl-2-pyrenedecanoylglycero-3-phosphomethanol (Molecular Probes), 250 μg of BSA (Sigma), 0.1 M NaCl, 0.25 mM $CaCl_2$, and 50 mM Tris buffer at pH 8.5 and 23 °C (*20*, *21*). The assay mixture was preequilibrated for 2−3 min to stabilize the baseline before the addition of the aliquot from the alkylation solutions. Residual activity was detected as an increase in the fluorescence at 396 nm (excitation at 345 nm on SLM 4800S spectrofluorometer) at each time interval.

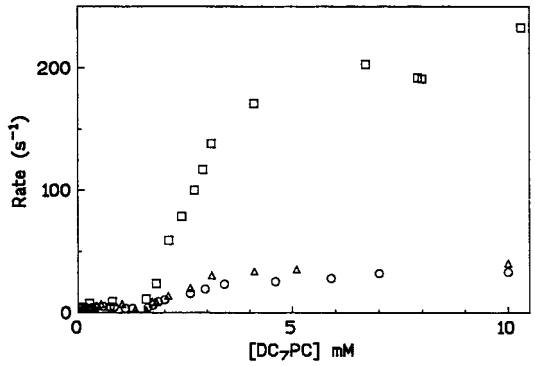

FIGURE 1: Dependence of the observed initial rate of hydrolysis as a function of the bulk [DC_7PC] by bovine PLA2 at pH 8.0 in 10 mM $CaCl_2$ and 0.1 M NaCl: (○) WT, (△) K56E, and (□) K53M. The cmc of DC_7PC is 1.5 mM under these conditions. For the results with K56M see Figure 2B.

Measurement of K_d (E to E) and K_d^I (E*I to EI).* The dissociation constant, K_d, was calculated from the binding isotherm obtained by monitoring the change in the tryptophan-3 fluorescence emission at 333 nm of PLA2 as a function of bulk deoxy-LPC concentration (*5*).

RESULTS

The interfacial kinetic behavior of PLA2 and its K56 and K53 mutants with DC_7PC micelles is compared. A marked quantitative difference at low [NaCl] is seen with the K53M and K56M mutants, yet the kinetic behavior is comparable at high [NaCl] or on anionic DMPM vesicles. Detailed kinetic analysis shows that residues 53 and 56 are critical for the salt-induced k^*_{cat} activation of pancreatic PLA2.

Rate of Hydrolysis of DC_7PC above the cmc Is Higher for K53M and K56M. The relationship between the bulk [DC_7PC] and the initial rate of hydrolysis by PLA2 is complex and depends on [NaCl] (*6, 9*). Except for significant quantitative differences, the shape of the rate versus [DC_7PC] profile at 0.1 M NaCl is qualitatively similar for WT, K56E, K53M (Figure 1), and K56M (Figure 2B). The magnitude of the maximum rate above the cmc depends on added [NaCl]. The maximum rates of hydrolysis at 0.1 M NaCl for the mutants differ by a factor of 10 in the order K56M > K53M > K56E > WT. The increase at 4 M NaCl is significantly larger for WT (Figure 2A) than it is for K56M (Figure 2B), and the maximum rates at 4 M NaCl are within a factor of 2 for these mutants, i.e., added NaCl effectively reduces the apparent kinetic difference between the WT and the mutants. In other words, higher rates seen with K53M or K56M mutants at 0.1 M NaCl do not increase as much at 4 M NaCl as the rates of WT and K56E.

The DC_7PC concentration at which the rate of hydrolysis increases sharply (Figures 1 and 2) corresponds to the cmc value. It does not change noticeably in the presence of the enzymes; however, it shifts to lower concentrations with added NaCl due to hydrophobic salting out. This is consistent with independent measurements of surface tension, which show that the cmc of DC_8PC-ether does not change significantly in the presence of pig (*6*) or bovine PLA2. Also, the cmc and the NaCl-induced changes in the rate profiles are in agreement with the cmc values measured as the inflection in the surface tension versus log [DC_7PC] in the aqueous subphase (*6, 22*).

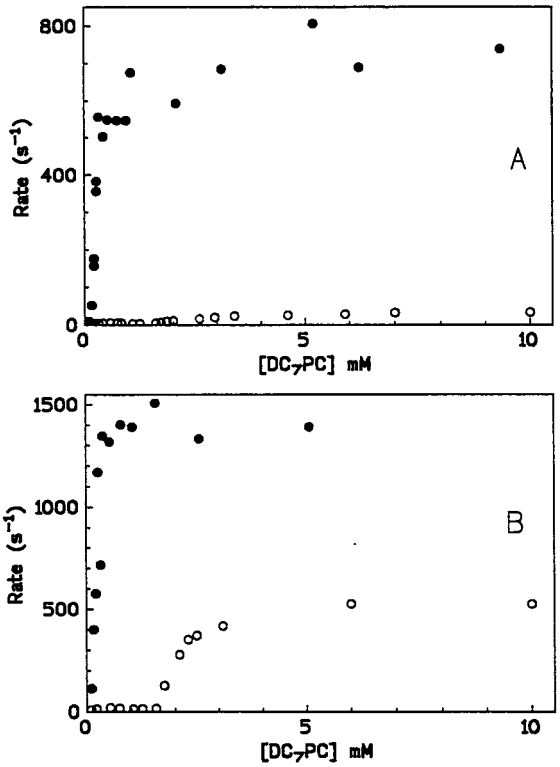

FIGURE 2: Effect of added NaCl on the dependence of the observed initial rate of hydrolysis on bulk [DC_7PC] by bovine PLA2 (A) WT and (B) K56M at pH 8.0 in 10 mM $CaCl_2$ in the presence of (○) 0.1 M and (●) 4 M NaCl.

The fact that the cmc values are not affected by WT and the K53 and K56 mutants at low and high [NaCl] suggests that the change in the observed rate above the cmc is due to a change in the bulk behavior of DC_7PC, i.e., the rate enhancement is due to a process associated with the micellization of the bulk substrate. In terms of our kinetic model (Scheme 1), the process is the binding of PLA2 to micelles whose concentration increases with bulk [DC_7PC]. Note that the apparent binding depends on the subsequent equilibria at the interface (*3*−*6*). As described below, the analysis of the apparent kinetic parameters shows the effect of NaCl on DC_7PC hydrolysis is in part due to the salting out of the enzyme into the interface. This effect accounts for the steepness of the micellar substrate concentration dependence in Figures 1 and 2, but the differences in the maximum rate, presumably seen when all the enzyme is bound to the interface, are attributed to a salt-dependent change in k^*_{cat}.

A monotonic increase in the observed rate with [NaCl] at 3.1 mM DC_7PC is seen with all the enzymes (Figure 3). These results showed that for all mutants the effect of NaCl is virtually the same at 1 and 100 mM, which rules out a simple electrostatic basis for the salt effect. Although the rates at low [NaCl] are different for the mutants, the observed rates at the maximum [NaCl], the solubility limit, do not appear to saturate. This would be expected if the [DC_7PC] at 3.1 mM remains subsaturating. However, at 4 M NaCl the apparent binding of the enzyme saturates at >2.5 mM DC_7PC (Figure 2), while the maximum rate continues to increase at 4 M NaCl (Figure 3). Thus the salt effect on the apparent maximum rate does not saturate at 4 M NaCl. In the following studies we have characterized the salt effect

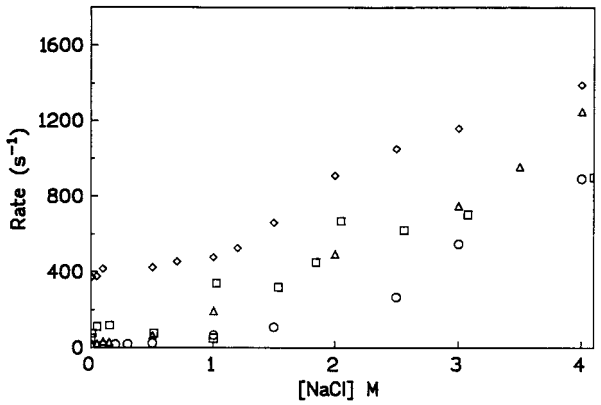

FIGURE 3: Effect of added [NaCl] on the observed initial rate of hydrolysis of 3.1 mM DC_7PC by bovine pancreatic PLA2: (○) WT, (□) K53M, (◇) K56M, and (△) K56E.

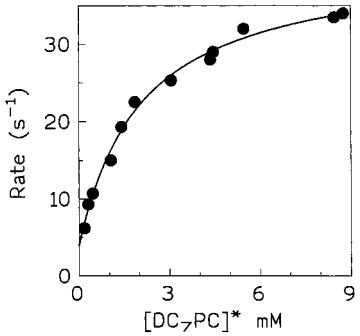

FIGURE 4: Dependence of the observed initial rate of hydrolysis as a function of bulk micellar [DC_7PC]* by WT PLA2 in 0.1 M NaCl and 10 mM $CaCl_2$ at pH 8.0. The apparent kinetic parameters derived from fit of such plots to eq 1 are summarized in Table 1 and interpreted in the text according to eqs 2 and 3. The micellar substrate concentration is obtained by subtracting the cmc from the bulk [DC_7PC].

by comparing the kinetic and binding parameters at low (0.1 M) and high (4 M) NaCl. Results show an effect of NaCl on k^*_{cat}.

Added NaCl Changes the Apparent Kinetic Parameters, K_M^{app} and V_M^{app}. The observed rate of hydrolysis above the cmc is sum of the rate of hydrolysis through the monomer path (including the reaction at the vessel walls) and through the interfacial path via the E*S complex on micelles (Scheme 1). The rate above the cmc increases with the fraction of PLA2 in the bound (E* + E*S) form, which increases with the bulk concentration of micellar DC_7PC. The rate of hydrolysis through the monomer path is given by V^{mono}. Thus three parameters are obtained from the hyperbolic dependence of the bulk substrate concentration present as micelles, [S*]:

$$v = \frac{(V_M^{app}[S^*] + V^{mono} K_M^{app})}{([S^*] + K_M^{app})} \quad (1)$$

As is the case in Figure 4, all mutants showed a reasonable nonlinear regression fit to eq 2 with $r^2 > 0.95$ and <30% standard deviation in values of K_M^{app} and V_M^{app} (Table 1). The apparent parameters show a clear effect of the K53 and K56 substitution and [NaCl]. For WT, the K_M^{app} decreases and V_M^{app} increases at 4 M NaCl. In 0.1 M NaCl, compared to WT, K_M^{app} is significantly lower for K56M. On the other hand, in 4 M NaCl, for all mutants K_M^{app} and V_M^{app} values

Table 1: Apparent Parameters for Bovine PLA2 and Mutants with DC_7PC

parameter	substrate	[NaCl] (M)	WT	K53M	K56M	K56E
V_M^{app} (s^{-1})	DC_8PM	0.1	850	850	630	700
	DC_8PC	0.1	135	400	420	300
	DC_8PC	4	2000	1750	1650	2000
	DC_7PC	4	850	1100	1400	1200
	DC_7PC	0.1	38	230	400	45
	DC_6PC	0.1	10		80	
	DC_6PC	4	240		400	
	dithio-DC_7PC	0.1	3		25	
	dithio-DC_7PC	4	78		116	
K_M^{app} (mM)	DC_7PC	0.1	2.3	1.3	0.75	1.3
	DC_7PC	4	0.2	0.2	0.26	0.25
	dithio-DC_7PC	0.1	1.9		0.4	
K_d (mM)	deoxy-LPC	0.1	3.0	2.1	0.9	2.3
	deoxy-LPC	4	0.4	0.3	0.3	0.4
cmc (mM)	DC_6PC	0.1	16		16	
	DC_6PC	4	1.8		1.7	
	DC_7PC	0.1	1.55		1.55	
	DC_7PC	4	0.09		0.1	

are in a narrow range, as is also the case for the hydrolysis of DC_8PM in the absence of NaCl or of DC_8PC in 4 M NaCl. Although the magnitude of the NaCl-dependent increase in the rate the hydrolysis of zwitterionic DC_nPC depends on the chain length, note that the rate of hydrolysis of anionic DC_8PM micelles decreases about 20% in 4 M NaCl for all mutants. A similar salt effect is seen on the enzyme bound to DMPM vesicles (*10*). In short, the maximum rate of hydrolysis by WT and mutants at saturating micellar DC_n-PC is higher in 4 M NaCl, and the relative magnitude of the salt effect is considerably larger for WT than it is for K53M and K56M.

Note that at pH 8.0 with 1 mM NaCl the rate of hydrolysis above the cmc by WT is about 35 s^{-1}, compared to the rate of about 10 s^{-1} seen just below the cmc. On the other hand, at pH 6.5 the rate, both above and below the cmc, is about 15 s^{-1}, which is comparable to that seen with pig PLA2 (*6*). Since pig PLA2 contains R53, on the basis of the results with K53M mutant (Figure 1) we conclude that the post-cmc increase seen with bovine WT at pH 8 in 1 mM NaCl is due to the presence of the basic deprotonated form of K53; the protonated form at lower pH is comparable to the pig PLA2 with R53. In short, in the presence of a cationic residue in positions 53 and 56, the rates of hydrolysis above and below the cmc in the absence of added NaCl are virtually identical.

Rates of Hydrolysis below the cmc Are Uninterpretable. The rate of hydrolysis of DC_nPC by pancreatic PLA2 below the cmc is low, and the observed rates are usually within a factor of 2 of the V^{mono} values obtained from the fit to eq 1. Typically, under a variety of conditions V^{mono} rates show a small (about 2×) increase for K56M. An attempt to investigate the effect of added NaCl on V^{mono} with DC_6PC is shown in Figure 5. Its cmc of 16 mM in 0.1 M NaCl decreases to about 1.7 mM in 4 M NaCl. The V^{mono} values for DC_6PC with WT and K56M change by less than a factor of 2 in the presence of 4 M NaCl. Comparable results were obtained with DC_7PC. At low [NaCl] the rate of hydrolysis below the cmc of DC_7PC is relatively low compared to the rate above the cmc. The salt-dependent lowering of the cmc is also seen in the rate versus [DC_7PC] curves (Figure 2). Although there are indications that the rates below the cmc are marginally different for the various mutants, we refrain

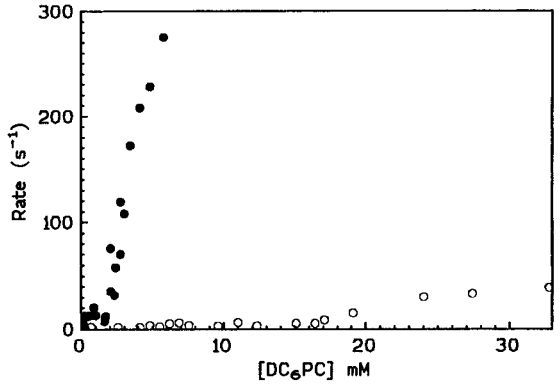

FIGURE 5: Dependence of the observed rate of hydrolysis as a function of DC_6PC by K56M PLA2 in (○) 1 mM NaCl or (●) 4 M NaCl. The points at longer times are not shown for clarity; however, see Table 1.

Scheme 3: Reaction Sequence for the Binding of PLA2 to a Neutral Diluent, Deoxy-LPC, Followed by the Hydrolysis of the Substrate Partitioned in the Interface

$$\text{E + deoxy-LPC} \overset{K_d}{\rightleftharpoons} \text{E* + S} \underset{k_{-1}}{\overset{k_1}{\rightleftharpoons}} \text{E*S} \xrightarrow{k^*_{cat}} \text{E* + P}$$

from the interpretation of these results. We believe that these rates are not true monomer rates, and possibly they are artifacts of the hydrolysis occurring at the surface of the reaction vessel.

$$V_M^{app} = \frac{k^*_{cat}}{1 + K^*_M} \quad (2)$$

$$K_M^{app} = \frac{K_d K^*_M}{1 + K^*_M}\left(1 + \frac{K'_S}{K_M}\right) \quad (3)$$

Analysis of the Apparent Parameters. As defined in terms of the sequential equilibria in Scheme 3 and eqs 2 and 3 (*3*, *5*, *6*), the apparent kinetic parameters K_M^{app} and V_M^{app} are related to K_d and the interfacial Michaelis parameters K_M* and k^*_{cat}. Results analyzed below show that the effect of added NaCl and K56 mutation is on K_d and k^*_{cat} but not on K_M*.

Added NaCl Enhances the Binding of PLA2 to the Zwitterionic Interface. Both K_M^{app} and K_d decrease with added NaCl (Table 1). According to eq 3, the effect of NaCl on K_M^{app} could be on any one or all of the four parameters: K_d, the affinity of the enzyme for the zwitterionic interface; K_M*, the interfacial Michaelis constant; K_S', the cmc of the substrate; and K_M, the Michaelis constant for the turnover in the aqueous phase. K_M values cannot be obtained directly; however, as shown elsewhere for pig pancreatic PLA2 (*6*), the effect of added NaCl on the binding of DC_nPC-ether (K_S) is exactly compensated by the effect of NaCl on the cmc. If K_S' is approximately equal to K_M, the effect of NaCl on K_d should correspond to the change in K_M^{app}, provided the salt effect on K_M* is not significant.

K53 and K56 Mutation and Added NaCl Have Little Effect on K_M.* Changes in K_M* for micellar substrates with added NaCl or on mutation were evaluated by established methods (*3*, *6*, *19*). K_M* for several substrates, obtained from the K_I* and $X_I(50)$ values are compared in Table 2. Magnitudes of K_M* are comparable to the independently measured K_S*.

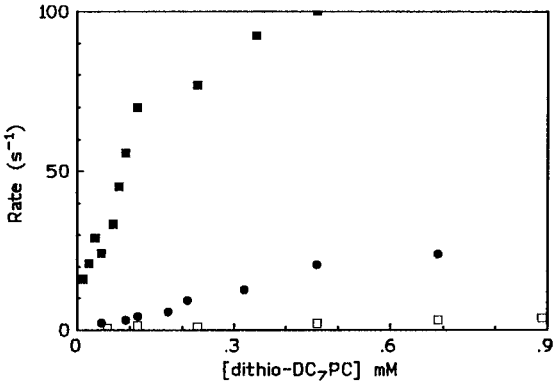

FIGURE 6: Dependence of the rate of hydrolysis of dithio-DC_7PC by K56M PLA2 in (■) 4 M NaCl or (●) 1 mM NaCl. The dependence for WT in 1 mM NaCl is also shown (□).

Table 2: $X_I(50)$ and K_M* for Bovine PLA2 Mutants with Micellar Substrates

substrate	inhibitor	[NaCl] (M)	parameter	WT	K53M	K56M	K56E
DC_6PC	MJ33	4	$X_I(50)$	0.01		0.007	
		4	K_M*	1.8		1.5	
DC_7PC	MJ33	0.1	$X_I(50)$	0.02	0.016	0.023	0.014
		0.1	K_M*	0.8	0.8	0.77	1
	RM2	4	$X_I(50)$	0.02	0.02	0.009	0.02
		4	K_M*	0.5	0.8	1.0	1.2
dithio-DC_7PC	MJ33	0.1	$X_I(50)$	0.03		0.035	
		0.1	K_M*	0.8		0.7	
DC_8PC	MJ33	0.1	K_M*	0.36	0.8	0.9	0.36
		4	K_M*	0.3	0.5	0.6	0.1
DC_8PM	MJ33	0.1	K_M*	0.01	0.03	0.01	0.02
		4	K_M*	0.04	0.025	0.02	0.03
DC_7PC-ether		0.1	K_S*	0.7		0.6	
		4	K_S*	0.45			

These results show that the effect of added NaCl and mutation on K_M* is marginal at best, which is consistent with the assertion that the effect of NaCl is through K53 and K56 residues.

Effect of [NaCl] on V_M^{app} Is Primarily on k^*_{cat}. According to eq 2, a marginal effect of NaCl on K_M* could not possibly account for a 5−60-fold change in V_M^{app} with added NaCl or mutation (Table 1). Even in the extreme outer range of the data, a change in K_M* from 0.3 to 1 would change k^*_{cat} by less than a factor of 2 (eq 2). We conclude that the increase in V_M^{app} at 4 M NaCl, is primarily due to an increase in k^*_{cat}, as also found to be the case with pig pancreatic PLA2 (*6*).

The only major change seen with K56M and K53M is in V_M^{app} at lower salt concentrations. Since K_M* changes little with added NaCl, we conclude that the effect of the mutation on k^*_{cat} is through a change in the fraction of the interfacial enzyme−substrate complex in the catalytically active form. As discussed below, this conclusion is consistent with a two-state model for k^*_{cat} allostery (Scheme 2), where the anionic charge in the interface stabilizes a rate-limiting intermediate $(E^*S)_a$ form by neutralizing the cationic charges of K53 and K56.

Chemical Step Remains Rate-Limiting. The rate of hydrolysis of dithio-DC_7PC by K56M shows a significant salt effect at the cmc (Figure 6). Note that the cmc and V_M^{app} values are significantly lower than those seen with DC_7PC under comparable conditions (Figure 2B, Table 1). The ratio of the rate with DC_7PC versus the rate with dithio-DC_7PC, the oxy/thio effect, remains around 10 for WT and K56M

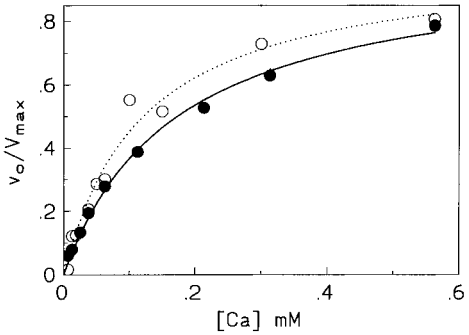

FIGURE 7: [Ca] dependence of the normalized rate of hydrolysis of (●) 10.5 mM DC_7PC and (○) 1.83 mM dithio-DC_7PC by K56M. The maximum rate of hydrolysis of the oxy substrate was about 10 times more than the rate with the thiosubstrate (= oxy/thio effect). The lines show the fit to a hyperbola that obtain kinetic $K^*_{Ca}(S) = K^*_{Ca}/(1 + 1/K_M^*)$, with $K^*_{Ca} = 0.35$ mM, was used for the calculation of K_M^* (*20*).

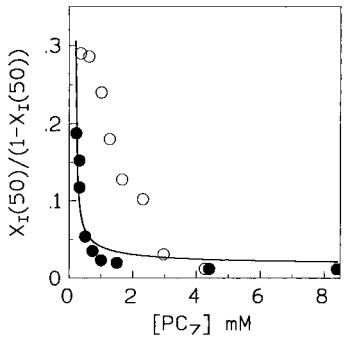

FIGURE 8: Dependence of the $X_I(50)$ for MJ33 as a function of micellar (●) [DC_7PC] and (○) [dithio-DC_7PC] by WT ppPLA2. The smooth line is drawn for eq 4 with $A = 2$ mM ($= K_M^{app}$); $B = 50$ [$= (1 + 1/K^*_I)/(1 + 1/K_M^*)$] with $K^*_I = 0.09$ mol fraction and $K_M^* = 0.7$ mol fraction; and $C = 1$; for details see ref *6*. These results for the oxy substrate are consistent with those obtained by other methods; however, the results for the thiosubstrate fit only at high substrate concentrations and low mole fractions of MJ33. The departure at low thiosubstrate concentration is attributed to nonideal mixing of MJ33 at higher mole fractions.

at the low and high [NaCl]. V_M^{app} is the rate at the maximum mole fraction of the substrate, $X_S = 1$, which by eq 2 is related to $k^*_{cat} = v_o(1 + K_M^*)$.

Results in Figure 6 show that, as is the case with DC_7PC, the rate of hydrolysis of dithio-DC_7PC increases at 4 M NaCl. K_M^{app} for the micellar thio substrate are marginally lower than those for the oxy substrate (Table 1), which suggests either that K_M^* and K_d are same for the two substrates or that they compensate for each other through other parameters. This is resolved by results in Figure 7, which show that the calcium concentration dependence for the hydrolysis of DC_7-PC and dithio-DC_7PC by K56M is almost the same. The apparent kinetic dissociation constant for calcium, $K^*_{Ca}(S) = 0.17$ mM, obtained from such a plot gives $K_M^* = 0.9$ mol fraction for DC_7PC, which compares favorably with $K_M^* = 0.6$ mol fraction for the thiosubstrate obtained from the other curve in Figure 7 (*20*). These results show that K_M^* for the oxy and thio substrates are comparable and that these values do not change on mutation or with added NaCl.

A complex relationship between $X_I(50)$ for MJ33 on the micellar oxy and thio substrate concentration is compared in Figure 8. It is analyzed in terms of eq 4 with the assumption that MJ33 is virtually completely partitioned into the interface (*6*). Values of the fit parameters for DC_7PC are $A = 2$ mM ($= K_M^{app}$), B = 55, and C = 12 with the cmc of 1.5 mM. At high [S*] the *B* term dominates and the relationship assumes the form for inhibition in the scooting mode (*3*). At this extreme substrate concentration, $X_I(50) = 0.02$ mol fraction for both the oxy and thio substrates, corresponding to $K_M^* = 0.8$ with $K_I^* = 0.009$. The *C* term dominates at low [S*] and a significant anomaly is seen with the thiosubstrate, which we attribute to the phase properties of the thiosubstrate which seem to change with mole fraction of MJ33.

Table 3: Equilibrium Binding and Catalytic Parameters for the Hydrolysis of DMPM by Bovine PLA2 and Mutants

parameter	WT	K53M	K56M	K56E
inactivation time for E (min)	0.6	1.5	0.6	1.3
K_{ND}* deoxy-LPC	>1	>1	>1	>1
v_o (s^{-1}) (DMPM at X_S=1)	330	260	250	230
K_{Ca} (mM) for ECa	0.5	0.2	0.3	0.3
K_{Ca}* (mM) for E*Ca	0.35	0.1	0.3	0.5
K_S* (E*CaDTPM)	0.02	0.12	0.01	>0.1
K_S* (E*CaDTPC)	>0.3	>0.3	0.1	0.08
K_{Ca}(DMPM)	0.12	0.08	0.1	0.3
K_M*	0.6	>1	0.7	1.4
K_P* (DMPM products)	0.02	0.06	0.014	0.06
K_M* (v_o/N_Sk_i)	0.4	1.6	0.25	1.7
K_I* (MJ33)	0.009	0.008	0.004	0.007
X_I(50)	0.023	0.011	0.015	0.008
K_M*	0.65	>1	0.42	>1
K_I* (RM2)	0.003	0.009	0.005	0.01
X_I(50)	0.016	0.011	0.012	0.012
K_M*	0.25	>1	0.7	>1
k^*_{cat} (s^{-1})	500	>500	300	>400

$$\frac{X_I(50)}{1 - X_I(50)} = \frac{[S^*] + A}{[S^*]B + AC - K_S(1 + 2A/[S^*])} \quad (4)$$

Collectively, these results show that K_M^* for the oxy and the thio substrates are comparable for WT and K56M. Therefore, the oxy/thio element effect is predominantly on k^*_{cat} at low and high [NaCl] (*14*). Since k^*_{cat} for the short-chain substrate changes without a change in K_M^*, and $K_M^* = K_S^*$ (Table 2), these results show that for bovine PLA2 $k^*_{cat} < k_{-1}$, where k_{-1} is the substrate dissociation constant for E*S (Schemes 2 and 3).

Turnover at the Anionic Interface Is Not Affected by Mutation. A full set of primary interfacial equilibrium binding and catalytic parameters for the three mutants at the anionic interface is compared in Table 3. These results clearly show that not only the rate of hydrolysis in the scooting mode on DMPM, but also the binding of the substrate, substrate analogues, products, and competitive inhibitors is comparable for WT and the three mutants. This is an expected result because under these conditions the bound enzyme sees only the anionic interface.

DISCUSSION

The catalytic efficiency of pancreatic PLA2 at the zwitterionic interface is modest at best, and an activating effect of the interfacial anionic charge is well established (*2, 4*). Relevance of the effect of interfacial anions bears on the fact that the physiological environment for the digestive action of pancreatic PLA2 includes bile salts. The biophysical basis for the role of the bile salt can now be dissected. As amphiphiles, bile salts solubilize the dietary substrate. Not only is PLA2 binding to these anionic mixed micelles

enhanced, but interfacial anionic charge has the k^*_{cat} allosteric effect. Note that monomeric bile salts do not enhance the hydrolysis via the monomeric Michaelis complex in solution (unpublished observations), which emphasizes the indispensable role of the interface in k^*_{cat} activation by interfacial anions.

The presence of cationic 53 and 56 residues in pancreatic PLA2, but not in some of the snake venom enzymes (*15, 24*), implies a functional significance in terms of their kinetic differences at the zwitterionic interface (*25*) but not at the anionic interface (*17*). A regulatory role for the cationic residues 53 and 56 is indicated by the fact that these residues are found in all pancreatic enzymes (type I) and also in the inflammatory PLA2 (type II). Unlike the venom enzymes, the pancreatic enzyme must select its target without damaging the surrounding tissues. A consensus on a specific mechanistic role for K53 and K56 has not emerged so far (*16*−*18, 26*); however, it is clear that K53 and K56 are at the extreme edge of the interfacial recognition region (i-face) along which PLA2 binds to the interface (*27*−*29*). On the other hand, many of the snake PLA2s, which lack the basic residues in consensus positions 53 and 56 (*15, 24*), do not exhibit a requirement or a preference for the anionic interface for catalysis (*30*) or binding (*31*); also, the salt-induced activation is not seen with these enzymes at the zwitterionic interface (unpublished observations).

Having resolved parallel kinetic effects of the interfacial anionic charge on K_d and k^*_{cat}, results in this paper show that a charge neutralization of K53 and K56 by the anion at the interface leads to k^*_{cat} activation. In addition to a modest effect on K_d, the major effect of K53M and K56M substitution is on k^*_{cat} at the zwitterionic interface at low salt concentrations. The effect of K53 and K56 substitution on k^*_{cat} and K_d is not seen at the anionic interface nor at the zwitterionic interfaces at high [NaCl].

To account for the effect of added NaCl on PLA2-catalyzed hydrolysis at zwitterionic interfaces we have identified several possibilities (*6*): (a) salt-induced hydrophobic effect on the protein, i.e., salting out of PLA2 into the interface, which will influence K_d; (b) selective partitioning of anions over cations, which will cause a biphasic increase in the net negative charge in the interface (*8*); (c) a direct allosteric effect of the interfacial anionic charge on k^*_{cat}. Enhanced hydrolysis seen with K56M and K53M at low [NaCl] suggests that the charge neutralization on these two residues is a critical part of the k^*_{cat} activation. As developed below, results are consistent with a model for k^*_{cat} allostery, in which the equilibrium between a catalytically active and an inactive form of E*S on the way to E* + P depends on the charge state of these two residues (Scheme 2).

k^*_{cat} Allosteric Modulation by the Interfacial Negative Charge. Results in Figures 1 and 2 clearly show that a large effect of added salt is on V_M^{app} for the turnover at the interface. V^{mono} for the turnover with monodisperse substrate is not noticeably affected in the presence of added NaCl or deoxycholate. Within the constraints of the general kinetic model for interfacial catalysis (Scheme 1), the effect on k^*_{cat} would be on the stabilization of any of the species between E*S and E*P along the reaction coordinates, which include a near-attack conformation, tetrahedral intermediate, and the transition state. Results with mutants support the assumption that the anion binding is to a site on E* or E*S. A monotonic increase in the rate with [NaCl] (Figure 3) suggests that the overall effect cannot be attributed in entirely to a change in the entropically driven surface electrostatics due to preferential partitioning of the anion over the cation in the interface, and more complex scenarios are not inconceivable. Although added NaCl must compete with ionic interactions between cationic PLA2 and anionic interface, the salting out effect of NaCl on PLA2 may also have a compensating effect. In short, in addition to the salting out of PLA2 to lower K_d, the effect of interfacial anion or of neutralization of K53 and K56 may be operationally viewed as a structural change that stabilizes a species between the substrate binding and the product release.

Structural Basis for k^*_{cat} Activation. A possible effect of salt on the pK_a of catalytic His-48 is ruled out by the fact that the inactivation kinetics of E and E* forms of PLA2 by phenacyl bromide is not influenced by 4 M NaCl. This is also consistent with the fact that K_I* and K_S* (=K_M*) change little with added NaCl or with K53 and K56 mutation, which leads to the conclusion that $k^*_{cat} < k_{-1}$. Similarly, there is little or no indication of a gross crystallographic conformational change on the binding of an inhibitor to the active site (*32*−*36*). Thus, effects leading to k^*_{cat} activation must be local and most likely associated with the presentation of the substrate in the active site for the chemical change.

The k^*_{cat} activation is due to the anionic charge at the interface. Electrostatic and hydrophobic interactions are involved in the binding of PLA2 to the interface (*27*−*29, 36*), although respective contributions are not quantitatively resolved. Multiple cationic residues are present on the face of PLA2 (i-face) that makes a contact with the interface. Besides K53 and K56, the cationic residues on the i-face include the α-amino group at the N-terminus (*37*), the 60−70 loop (*38*), and the C-terminus region with lysines at 113, 116, 120, and 121 (*39*). Allosteric and kinetic effect of substitution of these residues are under investigation; however, note that deletion of the seven residues at the C-terminus resulted in virtually total loss of activity on DC_8PC in 0.1 M NaCl ($V_M^{app} = 6\ s^{-1}$), yet at 4 M NaCl the rate of 1000 s^{-1} compares favorably to 1930 s^{-1} for WT (*39*).

Although the structure of PLA2 at interface is not available, several useful hints emerge from the crystal structure of K56M (*16*). As a first approximation, this structure may be taken as a charge neutralization mimic for WT at an interface. The backbone structure of WT and K56M are virtually identical; however, significant differences are found in the positions of residues 18−20, 29−32, and the 62−72 loop. Also, the orientation of the methionine side chain in K56M is quite different than that of the lysine in WT: a major change is in the χ^1 dihedral angle between C_α and C_1 from gauche$^-$ in WT to gauche$^+$ in K56M. As a result the 62−72 loop following the 41−58 helices is drawn closer. Interactions with the *sn*-3-phosphocholine group could become favorable in K56M because a hydrophobic pocket is generated with T52, A54, and M56 in the K56M mutant (*16*). This region also shows a change on molecular dynamic simulation of the enzyme binding the interface (*29*). Similar changes in WT on the binding to an anionic interface could provide a structural basis for removing the restraints on the catalytically inert form to make it functional (Scheme 2).

For the conceptualization of the difference between the $(E^*S)_i$ and $(E^*S)_a$ forms, we propose that the allosteric control of k^*_{cat} occurs via cationic residues 53 and 56. For example, this activation may involve events that relate to positioning of the *sn*-2 chain in the E*S complex. In the cocrystal structure of the substrate mimics in PLA2, the substituent at the *sn*-3-phosphocholine group is in the vicinity of K53 and K56 (*33*, *40*). K56 is on a helix that connects the 62−72 loop at the i-face (*41*) to the 40−52 helix. K53 is on the edge of the 41−52 helix that contains the catalytic residue H48, which acts as the general acid. In addition, the carboxylate of D49 provides two ligands for the binding of calcium (*27*, *36*), the obligatory cofactor for the substrate binding and the chemical step (*20*, *42*). The other five ligands around calcium include two water molecules (W5 and W12) and three ligands from the backbone carbonyls of residues 28, 30, and 32. In cocrystals of PLA2 with active-site-directed mimics, W5 is replaced by the *sn*-2 carbonyl oxygen. Also, the *pro-S* oxygen of the *sn*-3 phosphate replaces W12, and the ammonium group of the *sn*-3-phosphocholine is in close vicinity of K53, K56, Y52, and Y69. Thus K53 and K56 are potentially critical for fine-tuning the protein architecture and controlling the net charge in the catalytically important calcium binding region of PLA2, and the N-terminal helix along which the *sn*-2 chain of the substrate is oriented in the active site.

To recapitulate, equilibrium binding and kinetic parameters show that the effect of K56 and K53 mutation in PLA2 is not on the substrate binding as measured by K_M^* and K_I^*, which change little on mutation or added NaCl. From the Michaelis kinetic perspective it follows that the activation is in a step beyond the substrate binding, which by definition involves the transition state, intermediate and near-attack conformers. From the structural perspective, in analogy to parking brakes, in our conceptualization of k^*_{cat} allostery, the interfacial anion-induced changes in the K53 and K56 region coupled to the 60−66 loop may be responsible for changing the inert E*S to the active form.

REFERENCES

1. Gelb, M. H., Jain, M. K., Hanel, A. M., and Berg, O. G. (1995) *Annu. Rev. Biochem. 64*, 653−688.
2. Jain, M. K., and Berg, O. G. (1989) *Biochim. Biophys. Acta 1002*, 127−156.
3. Berg, O. G., Yu, B.-Z., Rogers, J., and Jain, M. K. (1991) *Biochemistry 30*, 7283−7297.
4. Jain, M. K., Gelb, M. H., Rogers, J., and Berg, O. G. (1995) *Methods Enzymol. 249*, 567−614.
5. Jain, M. K., Yu, B.-Z., and Berg, O. G. (1993) *Biochemistry 32*, 11319−11329.
6. Berg, O. G., Rogers, J., Yu, B., Yao, J., Romsted, L. S., and Jain, M. K. (1997) *Biochemistry 36*, 14512−14530.
7. Jain, M. K., Yu, B.-Z., Rogers, J., Ranadive, G. N., and Berg, O. G. (1991) *Biochemistry 30*, 7306−7317.
8. Tatulian, S. A. (1983) *Biochim. Biophys. Acta 736*, 189−195.
9. de Haas, G. H., Bonsen, P. P. M., Pieterson, W. A., and Van Deenen, L. L. M. (1971) *Biochim. Biophys. Acta 239*, 252−266.
10. Jain, M. K., Rogers, J., Berg, O., and Gelb, M. H. (1991) *Biochemistry 30*, 7340−7348.
11. Cajal, Y., Rogers, J., Berg, O. G., and Jain, M. K. (1996) *Biochemistry 35*, 299−308.
12. Cajal, Y., Ghanta, J., Surolia, A. K., Easwaran, E., and Jain, M. K. (1996) *Biochemistry 35*, 5684−5695.
13. Cajal, Y., and Jain, M. K. (1997) *Biochemistry 36*, 3882−3893.
14. Jain, M. K., Rogers, J., Gelb, M. G., Tsai, M.-D., Hendrickson, E. K., and Hendrickson, S. (1992) *Biochemistry 31*, 7841−7847.
15. Verheij, H. M., Slotboom, A. J., and de Haas, G. H. (1981) *Rev. Physiol. Biochem. Pharmacol. 91*, 91−203.
16. Noel, J. P., Bingman, C. A., Deng, T., Dupureur, C. M., Hamilton, K. J., Jiang, R., Kwak, J., Sekharudu, C., Sundaralingam, M., and Tsai, M.-D. (1991) *Biochemistry 30*, 11801−11811.
17. Lugtigheid, R. B., Otten-Kuipers, A. A. Verheij, H. M., and de Haas, G. H. (1993) *Eur. J. Biochem. 213*, 517−522.
18. Lugtigheid, R. B., Nicolaes, C. A. F., Veldhuizen, E. J. A., Slotboom, A. J., Verheij, H. M., and de Haas, G. H. (1993) *Eur. J. Biochem. 216*, 518−525.
19. Jain, M. K., Tao, W., Rogers, J., Arenson, C., Eibl, H., and Yu, B.-Z. (1991) *Biochemistry 30*, 10256−10268.
20. Yu, B.-Z., Berg, O. G., and Jain, M. K. (1993) *Biochemistry 32*, 6485−6492.
21. Yu, B.-Z., Ghomashchi, F., Cajal, Y., Annand, R. R., Berg, O. G., Gelb, O. G., and Jain, M. K. (1997) *Biochemistry 36*, 3870−3881.
22. Tausk, R. J. M., Karmigglt, J., Oudshoorn, C., and Overbeek, J. T. G. (1974) *Biophys. Chem. 1*, 175−183.
23. Rogers, J., Yu, B. Z., Serves, S. V., Tsivgoulis, G. M., Sotiropoulos, D. N., Ioannou, P. V., and Jain, M. K. (1996) *Biochemistry 35*, 9375−9384.
24. Van den Bergh, C. J., Bekkers, C. A. P. A., Verheij, H. M., and de Haas, G. H. (1989) *Eur. J. Biochem. 182*, 307−313.
25. Apitz-Castro, R. J., Jain, M. K., and de Haas, G. H. (1982) *Biochim. Biophys. Acta 688*, 349−356.
26. Cho, W., Tomasselli, A. G., Heinrickson, R. L., and Kezdy, F. J. (1988) *J. Biol. Chem. 263*, 11237−41.
27. Dijkstra, B. W., Drenth, J., and Kalk, K. H. (1981) *Nature 289*, 604−606.
28. Ramirez, F., and Jain, M. K. (1991) *Proteins: Struct., Funct., Genet. 9*, 229−239.
29. Zhou, F., and Schulten, K. (1996) *Proteins: Struct., Funct., Genet. 25*, 12−27.
30. Van Eijk, J. H., Verheij, H. M., Dijkman, R., and de Haas, G. H. (1983) *Eur. J. Biochem. 132*, 183−188.
31. Jain, M. K., Egmond, M. R., Verheij, H. M., Apitz-Castro, R. J., Dijkman, R., and de Haas, G. H. (1982) *Biochim. Biophys. Acta 688*, 341−348.
32. Scott, D., and Sigler, P. (1994) *Adv. Protein Chem. 45*, 53−88.
33. Thunnissen, M. M. G. M., Ab, E., Kalk, K. H., Drenth, J., Dijkstra, B. W., Kuipers, O. P., Dijkman, R., de Haas, G. H., and Verheij, H. M. (1990) *Nature 347*, 689−691.
34. Sekar, K., Eswaramoorthy, S., Jain, M. K., and Sundaralingam, M. (1997) *Biochemistry 36*, 14186−14191.
35. Dijkstra, B. W., Renetseder, R., Kalk, K. H., Hol, W. G. J., and Drenth, J. (1983) *J. Mol. Biol. 168*, 163−179.
36. Scott, D. L., Mandel, A. M., Sigler, P. B., and Honig, B. (1994) *Biophys. J. 67*, 493−504.
37. Maliwal, B. P., Yu, B.-Z., Szacinski, H., Squier, T., van Binsbergen, J., Slotboom, A. J., and Jain, M. K. (1994) *Biochemistry 33*, 4509−4516.
38. Kuipers. P., Dekker, N., Verheij, H. M., and de Haas, G. H. (1990) *Biochemistry 29*, 6094−6102.
39. Huang, B., Yu, B.-Z., Rogers, J., Byeon, I. J., Sekar, K., Chen, X., Sundaralingam, M., Tsai, M.-D., and Jain, M. K. (1996) *Biochemistry 36*, 12164−12174.
40. Scott, D., White, S. P., Otwinowski, Z., Yuan, W., Gelb, M. H., and Sigler, P. B. (1990) *Science 250*, 1541−1546.
41. Kuipers, O. P., Thunnissen, M. M. G. M., De Geus, P., Dijkstra, B. W., Drenth, J., Verheij, H. M., and De Haas, G. H. (1989) *Science 244*, 82−85.
42. Liu, X., Zhu, H., Huang, B., Rogers, J., Yu, B.-Z., Kumar, A., Jain, M. K., Sundaralingam, M., and Tsai, M.-D. (1995) *Biochemistry 34*, 7322−7334.

BI972896Z